Supporting Information

Defective PrO_x for efficient electrochemical NO_2^--to-NH_3 in a wide potential range

Shunhan Jia [1,2], Xingxing Tan [1,2], Limin Wu [1,2], Jiaqi Feng [1], Libing Zhang [1,2], Liang Xu [1], Ruhan Wang [1,2], Xiaofu Sun [1,2,*] and Buxing Han[1,2,3,*]

[1] Beijing National Laboratory for Molecular Sciences, CAS Key Laboratory of Colloid and Interface and Thermodynamics, CAS Research/Education Center for Excellence in Molecular Sciences, Institute of Chemistry, Chinese Academy of Sciences, Beijing, 100190, China

[2] School of Chemical Sciences, University of Chinese Academy of Sciences, Beijing 100049, China

[3] Shanghai Key Laboratory of Green Chemistry and Chemical Processes, School of Chemistry and Molecular Engineering, East China Normal University, Shanghai 200062, China

* Correspondence: sunxiaofu@iccas.ac.cn (X.S.); hanbx@iccas.ac.cn (B.H.)

Experimental Section

Materials

Praseodymium (III) chloride heptahydrate ($PrCl_3·7H_2O$), potassium nitrite (KNO_2), sodium salicylate ($C_7H_5NaO_3$), sodium hypochlorite solution (NaClO, 10%), sodium nitroferricyanide (III) dihydrate ($C_5FeN_6Na_2O·2H_2O$) were obtained from Innochem (Beijing) Technology Co., Ltd. Potassium hydroxide (KOH), sodium hydroxide (NaOH), potassium sulfate (K_2SO_4), hydrogen peroxide solution (H_2O_2, 30%), potassium chloride (KCl), ammonium chloride (NH_4Cl) were provided by Sinopharm Chemical Reagent Co., Ltd. Deionized (DI) water was used in the experiments. All the chemicals were used as received without further purification.

Catalyst preparation

To synthesize PrO_x-*T* (*T*=300, 500, and 700 ℃), its hydroxide precursor was prepared at first *via* a hydrothermal method reported in Ref. [1] with some modification. By adding 5 M KOH aqueous solution to 0.1 M $PrCl_3$ aqueous solution under stirring until $Pr(OH)_3$ precipitated completely, $Pr(OH)_3$ could be obtained after washing with DI water 5 times. 40 mL of 5 M KOH aqueous solution was added to $Pr(OH)_3$ precipitate, followed by a hydrothermal treatment for 48 h at 180 ℃. $Pr(OH)_3$ nanorods could be obtained after washing with DI water and dried in air at 60 ℃ overnight. $Pr(OH)_3$ nanorods were calcined at 800 ℃ for 2 h in the air for dehydration to Pr_6O_{11}. Followed by thermal treatment under 10% H_2/90% Ar atmosphere at different temperatures (*T*=300, 500, and 700 ℃) for 2 h, PrO_x-*T* could be obtained from Pr_6O_{11} for future utilization.

Characterizations

X-ray diffraction (XRD) analysis was performed on a Rigaku D/max-2500 X-ray diffractometer. Scanning electron microscopy (SEM) images were collected on a HITACHI SU8020 scanning electron microscope at an accelerating voltage of 5 kV. Transmission electron microscopy (TEM) images were acquired from a JEOL JEM-2100F high-resolution transmission electron microscopy. X-ray photoelectron spectroscopy (XPS) measurements were carried out on Thermo Scientific ESCA Lab 250Xi using utilizing 200 W monochromatic Al K radiation. Electron paramagnetic resonance (EPR) was conducted on a Bruker EMXplus-9.5/12. The absorbance data of the spectrophotometer was measured on a UV-vis spectrophotometer (Perkin Elmer, Lambda 1050+). The EPR spectra were recorded on a Bruker EMX-8 spectrometer.

Electrochemical measurements

Electrochemistry data was collected on CHI 630E electrochemical analyzer. NO_2^- reduction was carried out in 0.5 M K_2SO_4 aqueous solution with 0.01 M KNO_2 utilizing a typical H-cell (Gaossunion, C700-1) separated by a piece of Nafion 117 membrane under room temperature. Nafion 117 membrane was protonated with boiled water, 5% H_2O_2 solution, and 0.5 M H_2SO_4 solution, successively. A three-electrode configuration consisting of electrocatalysts loaded on carbon paper (1 mg cm^{-2}), Ag/AgCl reference electrode (with 3 M KCl solution), and Pt film counter electrode (1 cm^2) was used herein for electrochemical reactions. Current densities reported in this paper were recorded and normalized to the geometric area of the used electrode. All of the potentials for NO_2^- reduction were converted to a reversible hydrogen electrode (RHE).

Quantitative detection of NH_3

The salicylate method was used to quantify NH_3 in the catholyte [2]. Solutions 1, 2, and 3 were

prepared as follows. *Solution 1*: 0.32 M sodium hydroxide + 0.4 M sodium salicylate aqueous solution. *Solution 2*: 0.75 M NaOH + NaClO (active chlorine: 4.5%) aqueous solution. *Solution 3*: 10 mg mL^{-1} sodium nitroprusside aqueous solutions. To quantify the concentration of NH_3 in the catholyte, 5 ml of the aqueous sample solution, 1 mL of *Solution 1*, 0.1 mL of *Solution 2*, and 0.1 mL of *Solution 3* were sequentially added to a sample tube. The concentration absorbance curve was calibrated using the standard NH_4Cl solution with different NH_3 concentrations in 0.5 M K_2SO_4 and measuring the absorbance at 675 nm of the samples. A fitting curve (y = 0.00788x, R^2 = 0.99912) with ideal linear relation was calculated. The concentration of NH_3 in unknown samples was calculated through the absorbance at 675 nm and the fitting curve. Proton nuclear magnetic resonance (^1H NMR) spectra were obtained by a Bruker AV III 400 HD spectrometer after acidizing the solution to pH=2 with 5 M H_2SO_4.

Determination of NH_3 yield rate and Faradaic efficiency

NH_3 yield

$$NH_3 \text{ yield} = V \times C / (A \times t \times 17)$$

Faradaic efficiency (FE)

$$FE = 6 \times F \times V \times C / (Q \times 17) \times 100\%$$

where V was the volume of electrolyte; C was the concentration of generated NH_3; A was the active area of the electrode; t was the reaction time; F was the Faraday constant; Q was the electric charge.

Computational details

Spin-polarized first-principles calculations were performed by using the Perdew-Burke-Ernzerhof (PBE) exchange-correlation functional as implemented in the Vienna *ab initio* simulation package (VASP) [3,4]. The projector augmented wave (PAW) method and the corresponding pseudopotentials were employed. A cutoff energy of 500 eV was set for the plane wave basis set. The convergence thresholds for the energy and force are 10^{-5} eV and 0.02 eV/Å, respectively. The Grimme's DFT-D3 correction method was included to describe the weak dispersion interactions during surface adsorption. A 2 × 2 × 1 Monkhorst-Pack k-point sampling was set for all models [5].

The corresponding adsorption Gibbs free energies were then calculated as

$$\Delta G = \Delta E + \Delta \text{ZPE} - T\Delta S$$

where ΔZPE and ΔS are the changes in zero-point energy and in entropy, respectively, between the adsorbed state and free state, which can be obtained from the vibrational frequencies calculations (with adsorbates relaxed and substrates fixed) and standard thermodynamic data. T is the temperature.

Figure S1. Optical photograph of $Pr(OH)_3$ after hydrothermal treatment.

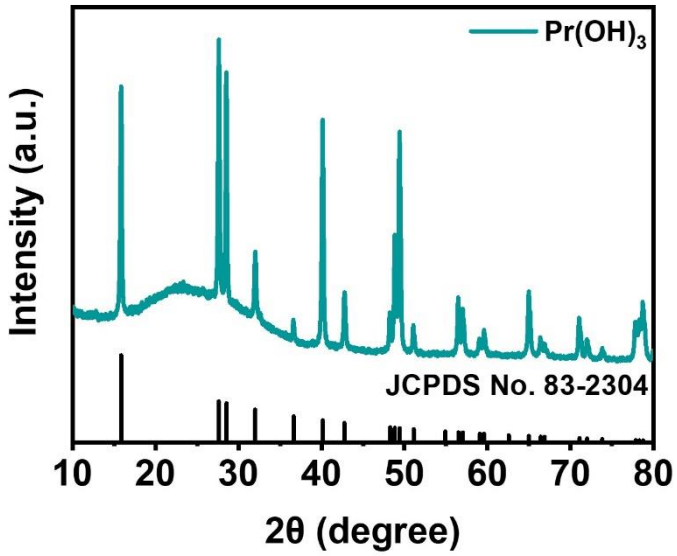

Figure S2. XRD pattern of $Pr(OH)_3$ obtained from hydrothermal method.

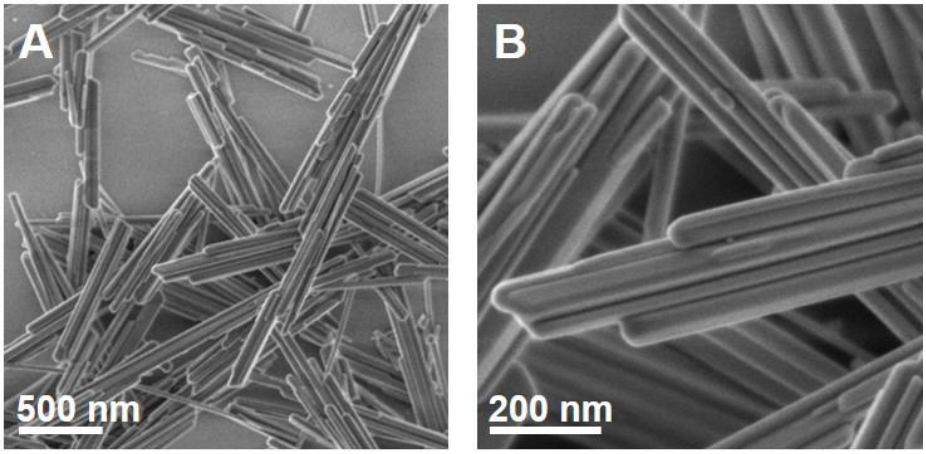

Figure S3. SEM images of synthesized $Pr(OH)_3$ nanorods.

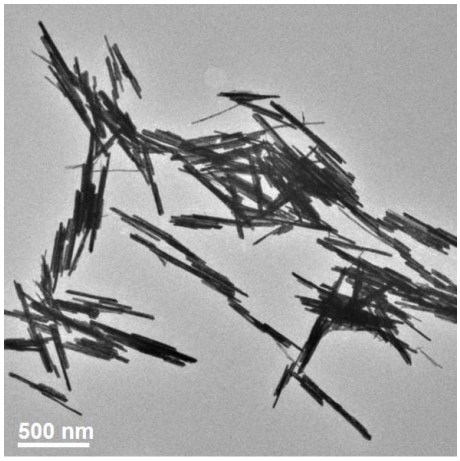

Figure S4. TEM image of $Pr(OH)_3$ nanorods.

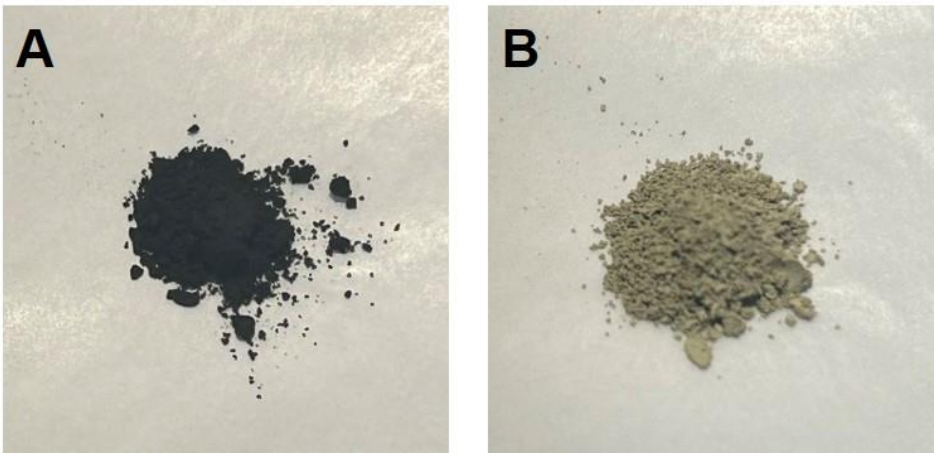

Figure S5. Optical photograph of (A) PrO_x-300 and (B) PrO_x-700 samples.

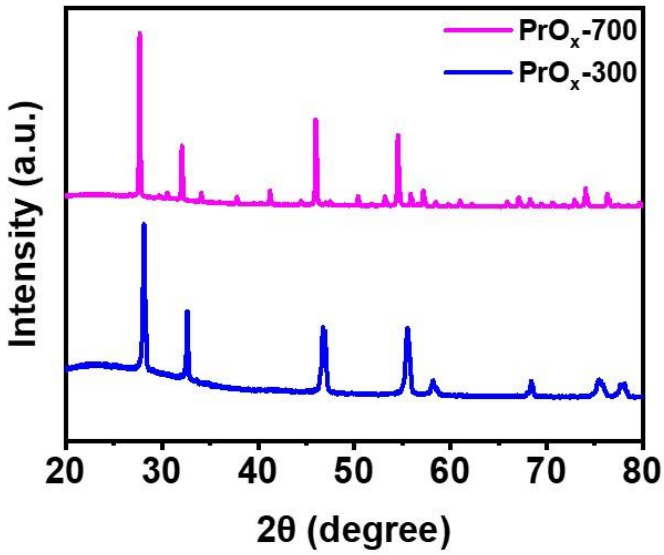

Figure S6. XRD patterns of (A) PrOx-300 and (B) PrOx-700.

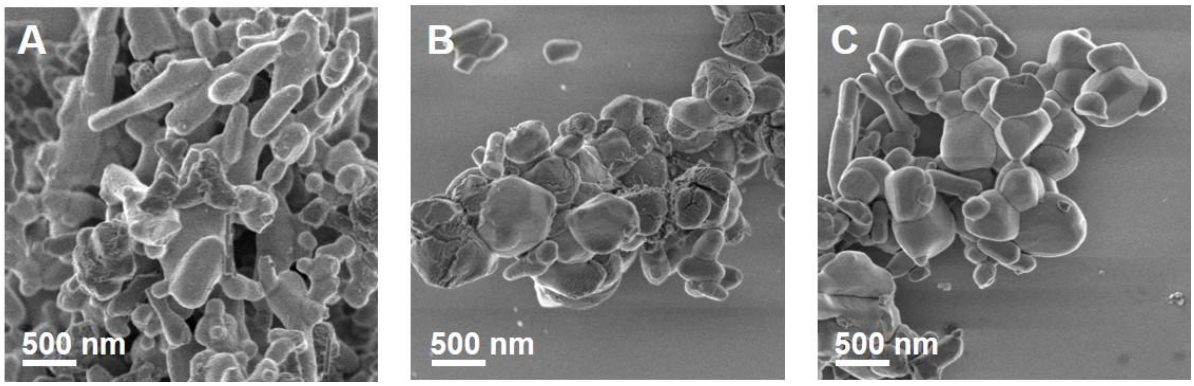

Figure S7. SEM images of the as-synthesized (A) Pr_6O_{11}, (B) PrO_x-300, and (C) PrO_x-700 samples.

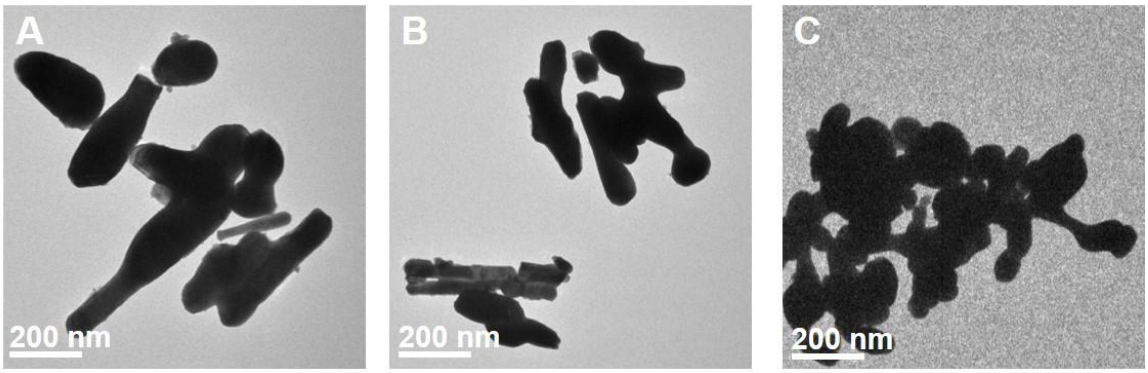

Figure S8. TEM images of the as-synthesized (A) Pr_6O_{11}, (B) PrO_x-300, and (C) PrO_x-700.

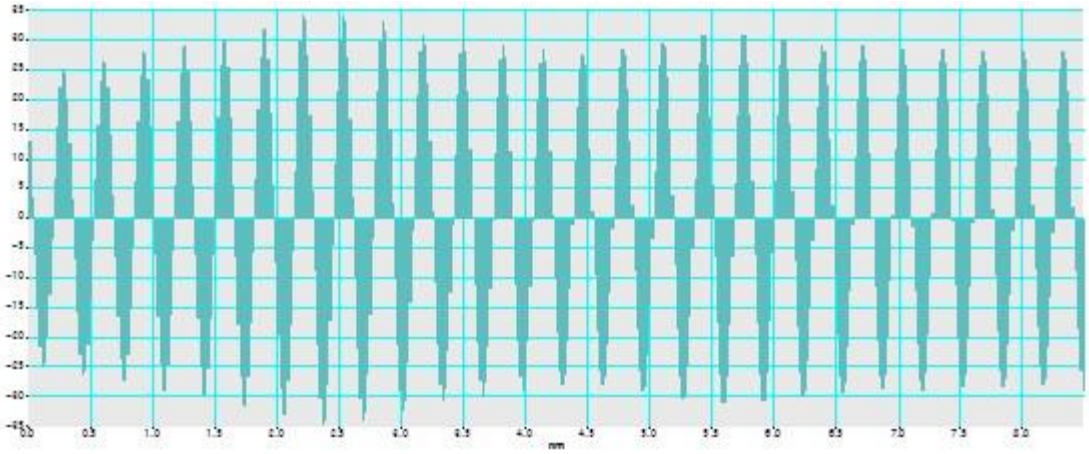

Figure S9. Well-resolved lattice fringe of PrO_x-500 in Figure 1D.

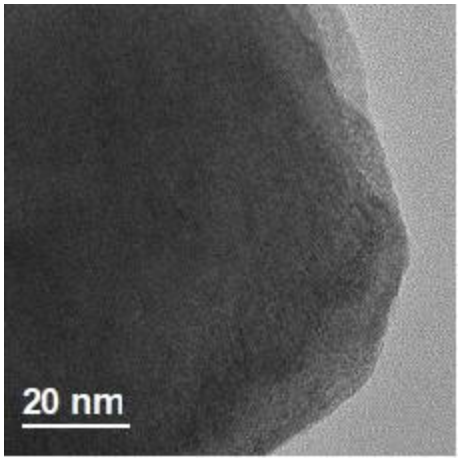

Figure S10. HR-TEM image of Pr_6O_{11}.

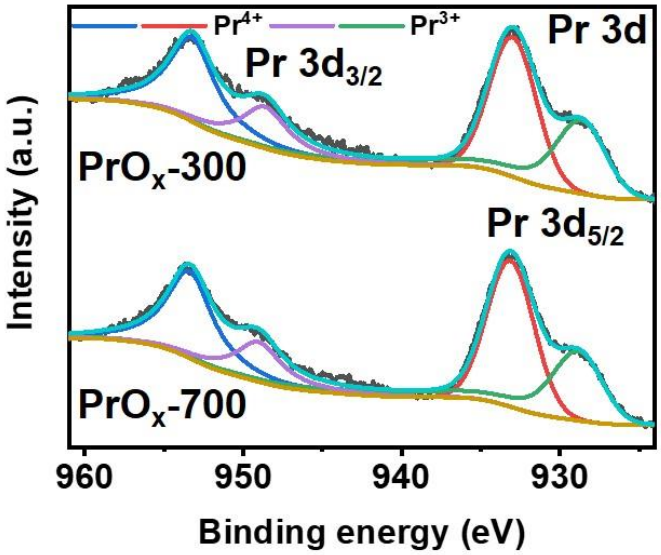

Figure S11. XPS curves of Pr 3d orbital of PrOx-300 and PrOx-700 surface.

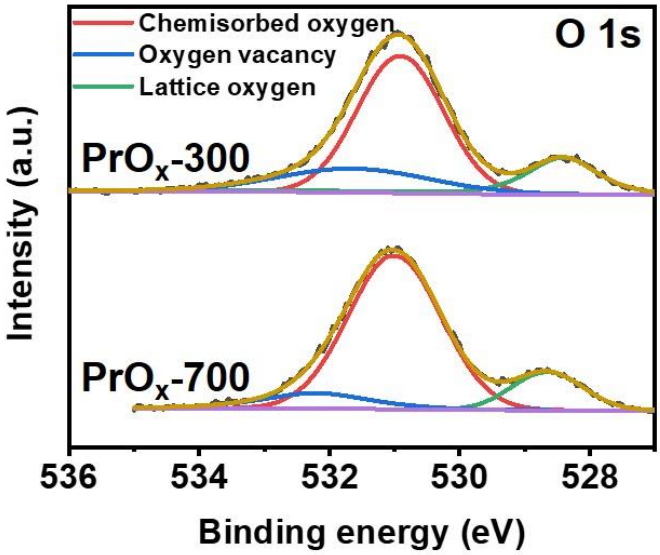

Figure S12. XPS curves of O 1s orbital of PrOx-300 and PrOx-700 surface.

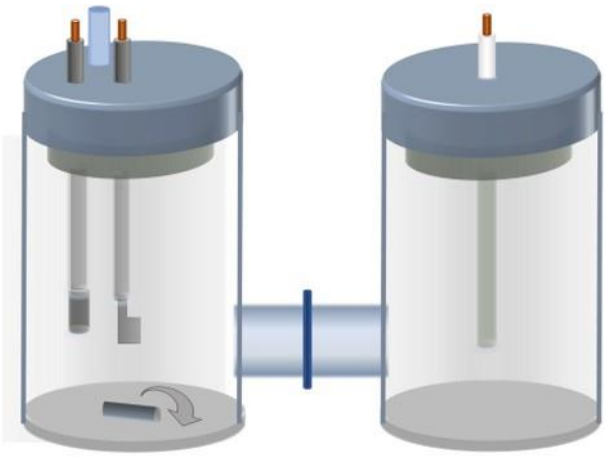

Figure S13. Illustration of H-cell used in this study.

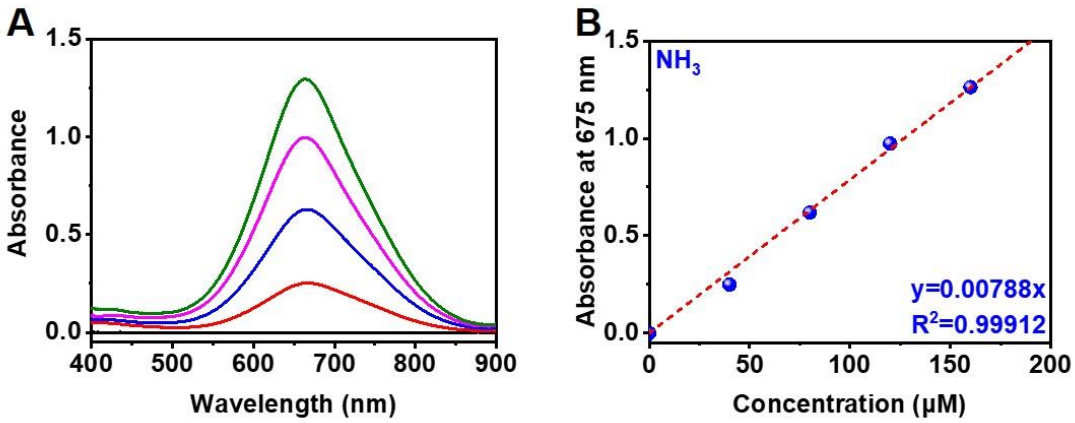

Figure S14. UV-vis absorption curves of indophenol assays kept with samples with different [NH_4^+] for at least 2 h at 25 ℃. (b) Calibration curve to estimate unknown [NH_4^+].

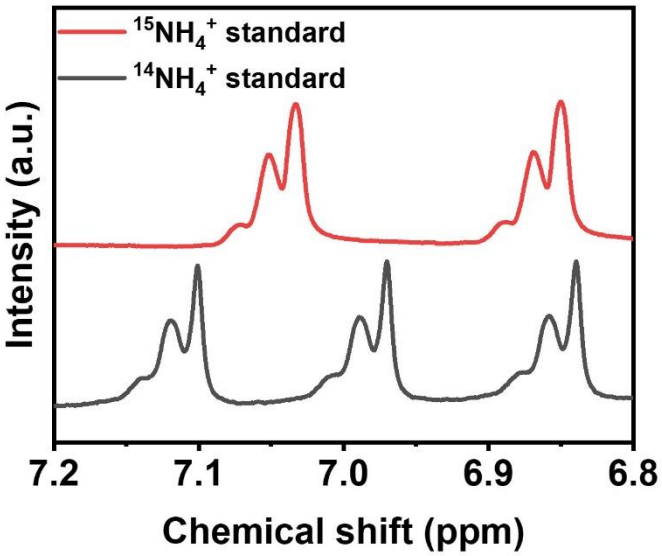

Figure S15. ^{1}H NMR spectra of $^{15}NH_4^+$ and $^{14}NH_4^+$ standard samples.

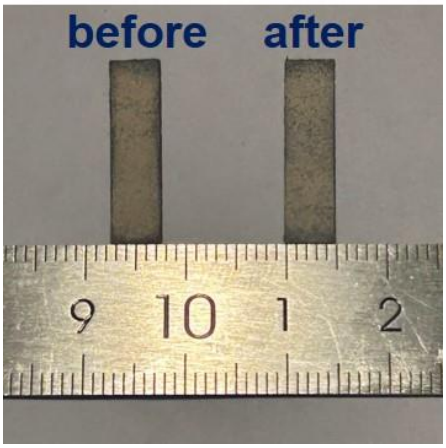

Figure S16. Optical photograph of working electrodes loading with PrO_x-500 catalysts before and after reactions.

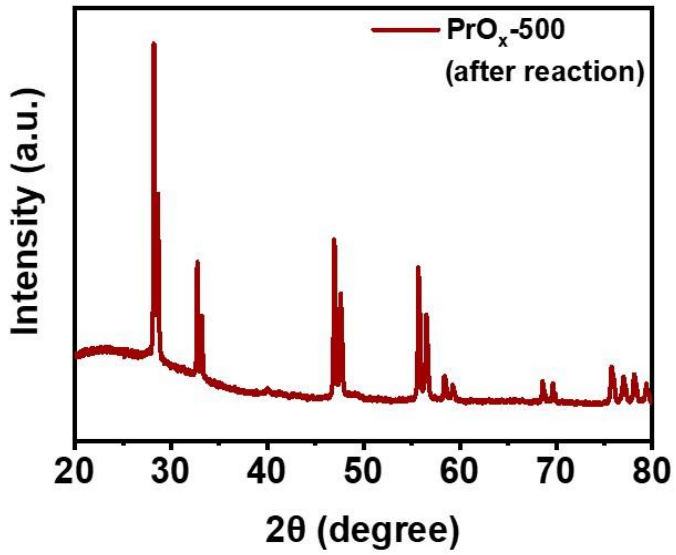

Figure S17. XRD pattern of PrO_x-500 after electrolysis.

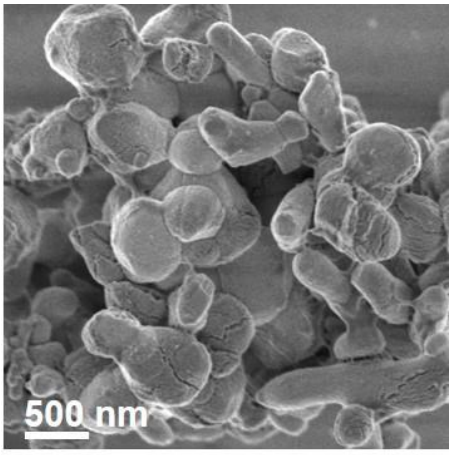

Figure S18. SEM image of PrO_x-500 after electrolysis.

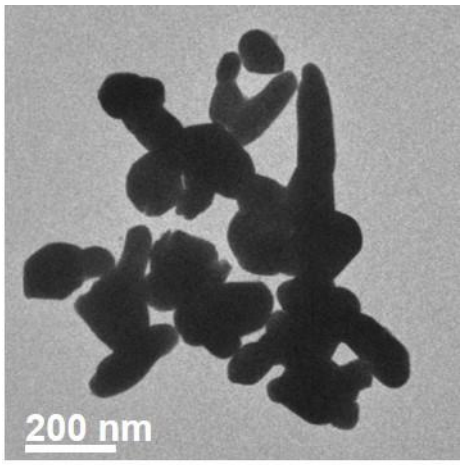

Figure S19. TEM image of PrO_x-500 after electrolysis.

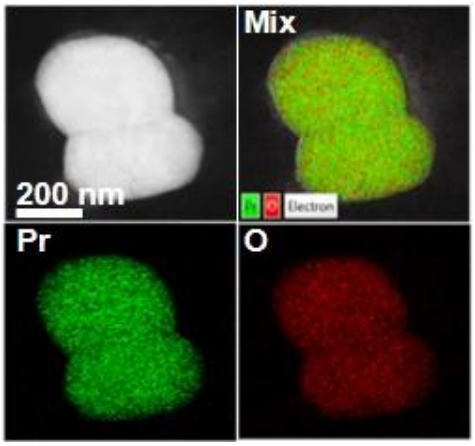

Figure S20. EDX mappings of PrO_x-500 after electrolysis.

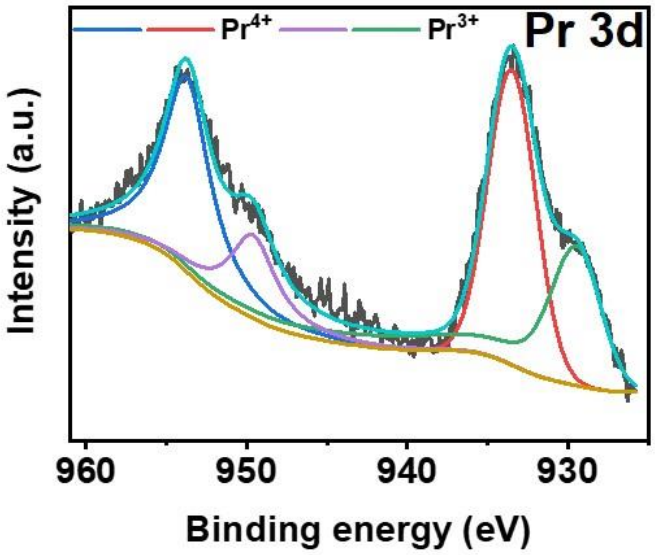

Figure S21. XPS curves of Pr 3d orbital of PrO_x-500 surface after reduction.

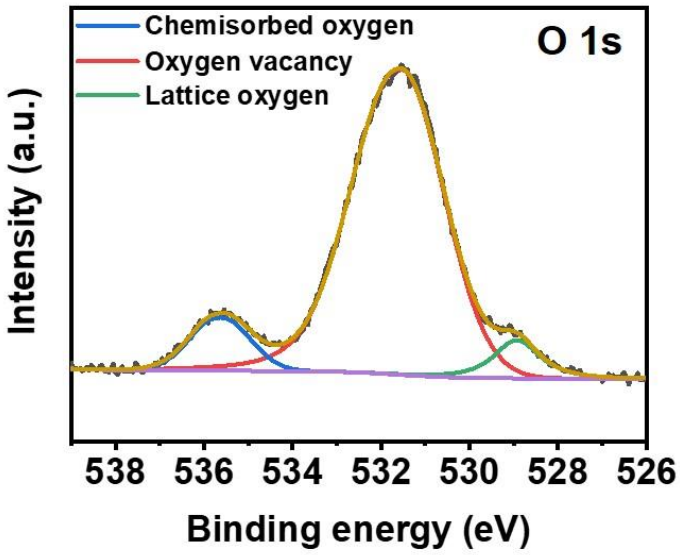

Figure S22. XPS curves of O 1s orbital of PrO_x-500 surface after reduction.

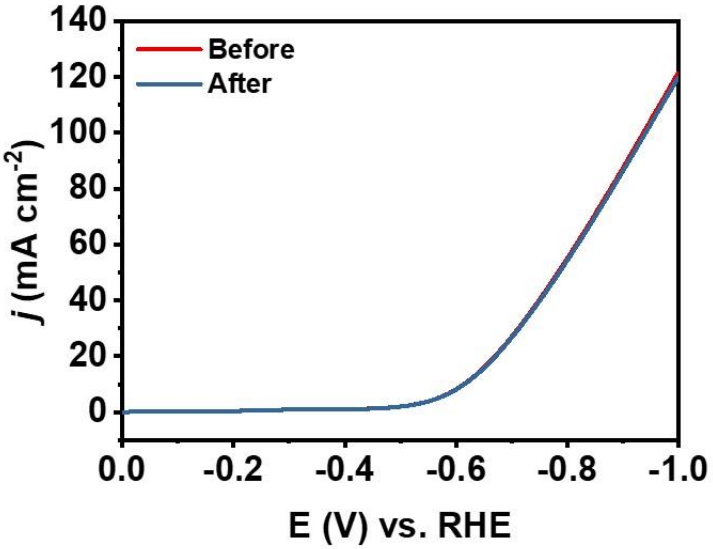

Figure S23. LSV curves of PrO_x-500 before and after reduction.

References

1. Huang, P.X.; Wu, F.; Zhu, B.L.; Li, G.R.; Wang, Y.L.; Gao, X.P.; Zhu, H.Y.; Yan, T.Y.; Huang, W.P.; Zhang, S.M.; et al. Praseodymium Hydroxide and Oxide Nanorods and Au/Pr6O11 Nanorod Catalysts for CO Oxidation. *J. Phys. Chem. B* **2006**, *110*, 1614-1620, doi:10.1021/jp055622r.
2. Wu, Y.; Jiang, Z.; Lin, Z.; Liang, Y.; Wang, H. Direct electrosynthesis of methylamine from carbon dioxide and nitrate. *Nat. Sustain.* **2021**, *4*, 725-730, doi:10.1038/s41893-021-00705-7.
3. Perdew, J.P.; Burke, K.; Ernzerhof, M. Generalized Gradient Approximation Made Simple. *Phys. Rev. Lett.* **1996**, *77*, 3865-3868.
4. Kresse, G.; Furthmuller, J. Efficient Iterative Schemes for Ab Initio Total-Energy Calculations Using a Plane-Wave Basis Set. *Phys. Rev. B Condens. Matter.* **1996**, *54*, 11169-11186.
5. Grimme, S.; Antony, J.; Ehrlich, S.; Krieg, H.A. Consistent and Accurate Ab Initio Parametrization of Density Functional Dispersion Correction (DFT-D) for the 94 Elements H-Pu. *J. Chem. Phys.* **2010**, *132*, 154104.